

## CHAPTER 12

### Violent Water Motion at Breaking-Wave Impact

M.J. Cooker\* and D.H. Peregrine†

#### Abstract

A numerical study of water waves breaking against a vertical wall is described. The exact equations for free-surface potential flow are solved. Solutions for a simple overturning wave meeting a vertical wall placed at several positions give unexpectedly violent water motion. The face of the incident wave can converge towards a point on the wall causing very high pressure, acceleration and velocity. It seems likely that this particular type of flow corresponds to the most extreme conditions encountered in laboratories and on coasts despite the lack of any direct water impact. Details of the flow reveal that compressibility of the water is unlikely to be relevant for wave forces, but that scaling from laboratory to prototype should allow for wall roughness and for small waves riding on the incident wave.

#### 1. Introduction

We describe results from a computational study of waves which are breaking or near breaking as they strike a vertical wall. Our aim has been to see how much information can be obtained about violent wave impacts, from a two-dimensional numerical model of irrotational inviscid flow. The model accurately deals with the overturning motion of a breaking wave and provides full information on velocities, pressures etc. up to the instant of impact.

A prototype example of the type of wave impact we envisage is sketched in figure 1. Shoaling water in front of a sea wall or breakwater causes an incident wave to break. Since such waves can cause appreciable damage many model experiments have been performed, e.g. Bagnold (1939), Nagai (1960), Mitsuyasu (1966), Richert (1968), Kirkgöz (1982), Chan & Melville (1988) and Partenscky (1988).

-----  
\*Research Assistant. †Professor.  
School of Mathematics, University of Bristol, University Walk,  
Bristol, BS8 1TW, England.

The underwater shape of the structure, or bed profile may cause the height/depth ratio of breaking waves to be much greater than that for a typical wave on a gently sloping beach. For example in some of Nagai's experiments the base of the vertical wall was exposed in front of some incident waves. This large height/depth ratio indicates that either the particular topography of an experimental or prototype structure should be modelled or an unconventional incident wave, much higher than the depth, should be used. We make the latter choice.

In addition we wish to study the effect of varying the distance between the wall and the breaking point of the wave. We do this by forming a wave which propagates over a flat horizontal bed. The initial wave has a gradual, monotonic increase in surface elevation. Hence, when it propagates, it steepens as the higher parts tend to catch up the lower portion of the wave. By choosing wave heights larger than 0.3 times the depth, the wave continues to steepen until it breaks. There is zero flow in front of this wave so that a vertical wall can be placed at any chosen spot in the path of the wave. This gives two primary parameters that may be varied:

- (i) the wave height
- (ii) the position of the wall relative to the position at which the wave would break in the absence of a wall.

In this paper, we consider a single wave height and look at variations of the wall position. Comparisons can be made with other types of wave by noting that our initial depth of water,  $h$ , corresponds to the depth of water in the *trough* of oscillatory waves, and not to the mean water level.

## 2. The mathematical and numerical model

The flow is assumed to be inviscid, two-dimensional and incompressible with irrotational flow so that a velocity potential satisfying Laplace's equation can be used. The effect of the air above the water is neglected, so that the free surface is at constant pressure. No further approximations are made in the mathematical formulation.

The numerical modelling is carried out with a program developed from the accurate and efficient, high-order, boundary-integral method of Dold and Peregrine (1986). Recent examples of work with closely related programs are Tanaka, Dold, Lewy and Peregrine (1987) and Cooker, Peregrine, Vidal and Dold (1990).

The initial wave, we have chosen, has a horizontal velocity

$$u(x,0) = -\frac{1}{2}u_0(gh)^{\frac{1}{2}}[1+\tanh \lambda(x-x_0)]$$

and elevation  $\zeta(x_0) = (|u_0| + \frac{1}{2}u_0^2)h$ .

This corresponds to a "simple-wave" solution of shallow-water theory for a wave propagating in the  $-x$  direction if the initial surface slope is gentle enough. Using units in which  $g$  and  $h$  are both unity, we illustrate results for the wave of height

$$\Delta h = \zeta(\infty, 0) - \zeta(-\infty, 0) = 1.5$$

(i.e.  $u_0 = 1.1623$ ). With  $\lambda = 0.5$ , there was no significant wave in the  $+x$  direction and the wave soon develops into a plunging breaker as shown in figure 2 where  $x_0 = 0$ . Although shallow-water theory guides our choice of initial conditions, the computations make no such simplifying assumptions.

A vertical wall can be inserted in this flow at any chosen place. In fact, the wall is modelled by using symmetry: two equal and oppositely-directed waves travel towards each other starting a distance  $x_0$  from the line of symmetry ( $x=0$ ). For example  $x_0 = 9$  gives a wall positioned at  $x = -9$  in figure 2, directly in the path of the overturning jet. On the other hand  $x_0 = 7.5$  places a wall close to the point where the wave first has a vertical tangent to its free surface.

For purposes of illustration just the one initial wave,  $\Delta h = 1.5$ ,  $\lambda = 0.5$ , is used with different values of  $x_0$ . This wave can be compared with other more realistic waves by noting that at the initial time there is no motion at the wall and water is moving towards the wall. Thus, our initial condition resembles an oscillatory or irregular wave at the moment its trough is adjacent to the wall. That means our depth  $h$ , corresponds to *minimum* water depth at the wall.

### 3. Examples of wave motion against a wall

First we consider the case  $x_0 = 9$  where an overturning wave meets the wall. This is illustrated in figure 3. As may be seen, the profile of the overturning part of the wave appears to be unaffected by the wall. Examination of the computed velocities and accelerations shows that the velocity of the jet is unchanged at  $2.6 (gh)^{\frac{1}{2}}$  and the horizontal acceleration under the jet, which is  $3.4g$  in the undisturbed wave, changes little. On the other hand, the part of the wave near the water-line cannot pass through the wall and *rises quickly up the wall*. For the last profile calculated the vertical velocity and acceleration at the wall are  $18.5 (gh)^{\frac{1}{2}}$  and  $17.5 g$ , respectively.

The current program is unable to model the direct impact of the jet on the wall (though see Cooker and Peregrine, 1990). However, experiments from those of Bagnold (1939) onwards, clearly show that maximum pressures occur if the wave has a vertical face when it meets the wall. Hence we could expect from figure 2 a value of  $x_0 = 7.5$  to give us a more severe impact.

As may be seen in the illustrations of figure 4(a) and (b) the wave with  $x_0 = 7.5$  fails to develop a vertical face, because of the proximity of the wall. The water surface rises smoothly and then forms a thin vertical jet at the wall, so no actual impact occurs. Except for the region near its base the jet is in free fall. Its velocity of  $14 (gh)^{\frac{1}{2}}$  indicates it could rise to a height of about  $100h$ . In practice its motion is likely to be disrupted by the air.

The flow at the base of the jet is interesting, especially at its inception. Here a maximum water acceleration of nearly  $2000g$  is computed and the correspondingly high pressure gradients lead to a brief high pressure on the wall, as the jet forms. The distribution of pressure on the wall at the time of maximum pressure is given in figure 5. Note how the pressure is significantly greater than instantaneous hydrostatic pressure all the way down to the bed. In figure 6 contours of pressure field throughout the water are shown. It can be seen that substantial pressures extend some distance from the wall.

From an engineering point of view it is the pressure distribution on the wall which is usually most relevant. This is plotted as a function of time in figure 7. Only a brief interval  $(-0.7 \text{ to } +0.045)(h/g)^{\frac{1}{2}}$  each side of the maximum is shown, but as may be seen this covers all the pressure greater than  $8\rho gh$ . The values that would be read by a fixed pressure gauge on the wall are easily deduced by looking along a horizontal line in the diagram.

As already noted the incident wave does not become vertical for  $x_0 = 7.5$ ; computations with  $x_0 = 8$  do give a vertical face. As shown in figure 8 this wave only briefly has a vertical face. The free surface flow is dominated by a convergence toward the wall. Again a jet forms. This example gives the most severe conditions we have computed so far. Compared with the case of  $x_0 = 7.5$  the greater convergence of the flow gives a smaller, more violent jet. Its velocity is  $20 (gh)^{\frac{1}{2}}$ , corresponding to a height of  $200h$  in free fall. The small jet size leads to greater computational effort being needed to resolve the motion. At the last reliably resolved time, pressure and acceleration are still increasing at levels in excess of  $50\rho gh$  and  $6000g$ , respectively. Maxima of over  $60\rho gh$  and  $8000g$  are expected. The maximum value of  $\partial p/\partial t$  has been calculated and is  $3000\rho g^{\frac{3}{2}}h^{\frac{1}{2}}$ , which gives a typical time scale for the pressure rise of about  $0.005(h/g)^{\frac{1}{2}}$ .

#### 4. Discussion

It has been a surprise that high "impact-type" pressures are found in a smooth potential flow. These pressures are of the same order of magnitude as the maximum pressures found experimentally for laboratory waves. As is well known these do not agree well with large-scale measurements when Froude scaling is used. Nevertheless we show in table 1, how our estimated maximum results scale for different heights of wave from laboratory to full-scale.

Table 1: Scaling of extreme conditions

Initial water depth	$h$	<u>50mm</u>	<u>100mm</u>	<u>1m</u>	<u>5m</u>
Total initial wave height	1.5h	75mm	150mm	1.5m	7.5m
Maximum velocity	$20(g/h)^{\frac{1}{2}}$	$14m\ s^{-1}$	$20m\ s^{-1}$	$60m\ s^{-1}$	$140m\ s^{-1}$
Maximum acceleration	8000g				
Maximum pressure (as a head of water)	$60\rho gh$	3m	6m	60m	300m
Time scale of pressure rise	$0.005(h/g)^{\frac{1}{2}}$	0.35ms	0.5ms	1.6ms	3.5ms

The maximum pressures occur while a jet forms from a flow which has converged towards a point on the wall. Experimental descriptions mention an impact of the vertical wave face, yet this does not occur, the water surface violently "flips through" from a contracting half-cavity to a high speed vertical jet. In a recent paper Chan and Melville (1988) observe from high-speed photography "that wave impact occurred through the focussing of the incident wavefront onto the wall; that is through a convergence of the wave crest and the surface intersection point at the wall"; a description which fits our results.

Hattori (private communication 1990) measures high impact pressures of  $120\rho gh$  in an experiment which looks similar to our computation. There is a trace of a jet in one of his video frames. However we expect the jet to be only 0.3mm thick and to form on a time scale of 0.3ms so it is not surprising that it is difficult to observe, for example Chan and Melville use film at 1100 frames per second, and Hattori's video is at 200 frames per second. Both these recent experiments were made on a scale where the incident wave was only a few centimetres high, and both measured highest peak pressures at the "flip through" condition.

Our results lead us to speculate that if the filling "cavity" contracts to a small enough size then there is no upper limit on pressure and jet velocity within our model. Clearly, neglected physical properties such as viscosity and compressibility might change this picture. Since we have full details of the potential flow it is easy to assess the relevance of these effects.

We have considered incident waves as low as 10mm high and estimate that the effects of surface tension and viscosity are unimportant until after the formation of the jet. Even then it is only in the jet that surface tension can be relevant. The major physical effects in this "flip through" motion are the fluid inertia and the pressures it generates. Once water is in the jet these hydrodynamic pressures become negligible so that we expect surface tension and aerodynamic effects to become important, e.g. thin jets rapidly break up into spray.

The role of compressibility has often been discussed in the context of water wave impact. In the most violent impact we have calculated, where no air is trapped, we have a maximum value of  $\partial p / \partial t = 3000 \rho g^{\frac{2}{3}} h^{\frac{1}{3}}$ . This can be used to compare terms in the continuity equation for a *compressible* fluid. We find the ratio

$$\frac{\partial p}{\partial t} / \rho \frac{\partial v}{\partial y} \approx 15 \frac{gh}{a^2}$$

where  $a^2$  is the velocity of sound.

A low value of  $a = 100 \text{ m sec}^{-1}$ , corresponds to water aerated with 1% by volume of small bubbles. Even then for  $h = 1 \text{ m}$  this ratio is 0.015. Hence compressibility has little effect on the fluid dynamics. However a loud noise only requires a small amount of energy compared with that in the water motion.

Although it is hard to compare prototype conditions with experiments it is generally considered that the Froude scaling, which is natural for relating our computations to physical reality, generally overestimates prototype pressures. Since compressibility and viscosity appear to be irrelevant for this scaling we consider a different possibility.

From our computations it appears that high pressures are obtained when the wave surface focusses toward a point before a vertical jet is formed. Superficially, there seems to be no limit to this focussing and hence to the maximum pressure. On the other hand finer focussing implies a smaller and more violent jet. The minimum size of coherent jet that can be created depends on the roughness of the wall and liquid surfaces involved, e.g. if a wall has a roughness of about 10mm amplitude then pressures computed for the generation of a jet of width 10mm at a smooth wall are likely to be gross over-estimates. Large waves almost always have smaller waves upon them, and this free surface "roughness" is also likely to influence the maximum pressures at a wall, by either disrupting the surface focussing or inducing premature jet formation.

One further unexpected feature is the large extent of short-lived pressures which are several times higher than the hydrostatic value. The bed experiences this pressure pulse and it is interesting to speculate on the response of sediments to such a loading.

## 5. Conclusion

Potential flow computations reveal that there is violent water motion and very high pressures when near-breaking waves meet a vertical wall. The highest pressure occurs when a high-speed vertical jet forms at the wall. It seems likely that this "flip-through" type of interaction between wave and wall can give higher pressures than a direct impact by the jet from an overturning wave. The computed results indicate that the compressibility of water is unlikely to be of any importance, but that roughness of the wall or water surface may be significant in limiting extreme pressures for coastal waves.

## References

- Bagnold, R.A. (1939) "Interim report on wave-pressure research". J.Inst. of Civil Engineers (1938-39), 12, p201-226.
- Blackmore, P.A. and Hewson, P.J. (1984) "Experiments on full-scale wave impact pressures". Coastal Engineering, 8, pp 331-346.
- Chan, E.S. and Melville, W.K. (1988) "Deep water plunging wave pressures on a vertical plane wall". Proc.R.Soc.Lond A417, 95-131.
- Cooker, M.J. and Peregrine, D.H. (1990) "A model for breaking wave impact pressures". Proc.22nd Intl.Conf.Coastal Eng. The Netherlands, June 1990.
- Cooker, M.J., Peregrine, D.H., Vidal, C. and Dold, J.W. (1990) "The interaction between a solitary wave and a submerged semi-circular cylinder". J.Fluid.Mech., 215, 1-22, Apr. 1990.
- Dold, J.W. and Peregrine, D.H. (1986) "An efficient boundary-integral method for steep unsteady water waves" in "Numerical methods for fluid dynamics II". Eds.K.W. Morton and M.J. Baines. Oxford.Univ.Press, 671-679.
- Kirkgöz, M.S. (1982) "Shock pressure of breaking waves on vertical walls". Eng.Div., Proc.ASCE, 108, Feb. 1982.
- Mitsuyasu, H. (1966) "Shock pressure of breaking waves I". Coastal Eng.Japan, 9, 83-96.

Nagai, S. (1960) "Shock pressures exerted by breaking waves on breakwaters". J. Waterways and Harbours Div. Proc., ASCE, WW2, 86, 1-38.

Partensky, H.W. (1988) "Dynamic forces due to breaking waves at vertical coastal structures". Proc. 21st Coastal Eng. Conf. June 1988, 2504-2518.

Richert, G. (1968) "Experimental investigation of shock pressures against breakwaters". Proc. 11th Conf. Coastal Eng. ASCE, 1, 954-973.

Tanaka, M, Dold, J.W., Lewy, M. and Peregrine, D.H.(1987) "Instability and breaking of a solitary wave". J.Fluid Mech.,185, 235-248.

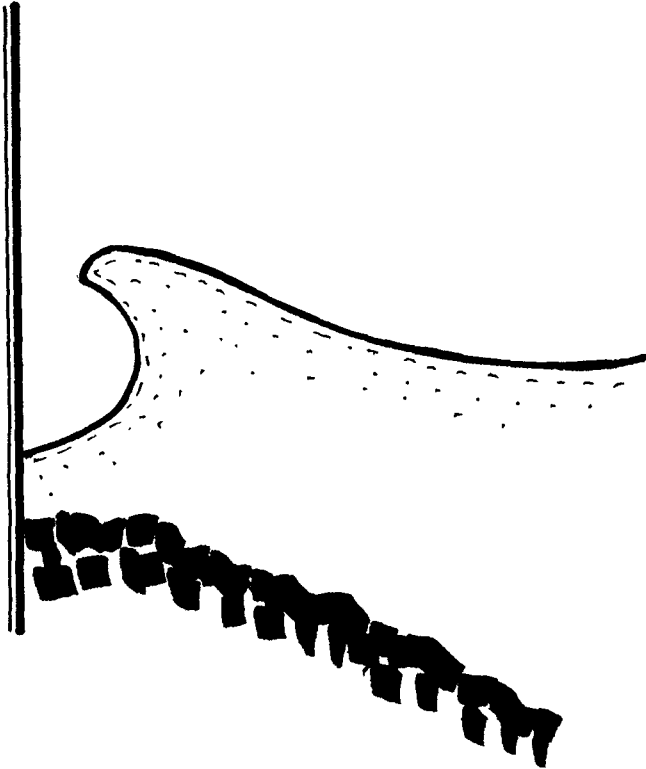


Figure 1: Sketch of a wave hitting a wall.

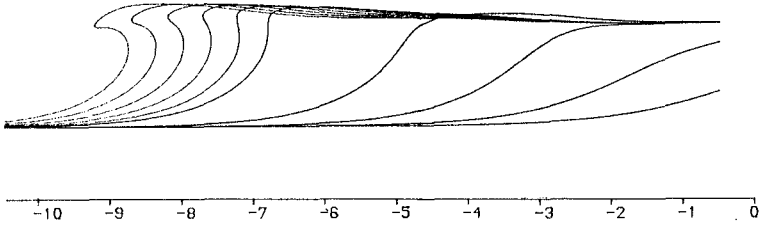


Figure 2: A wave of height  $1.5h$  advancing into still water of depth  $h$  *without any wall*. The free-surface profiles are at times  $t = 0$  (1) 4 (0.2) 5  $\sqrt{(h/g)}$ . The maximum velocity in the jet is  $2.6 \sqrt{(gh)}$ . The steady flow at  $x = +\infty$  has speed 1.162, and is directed to the left.

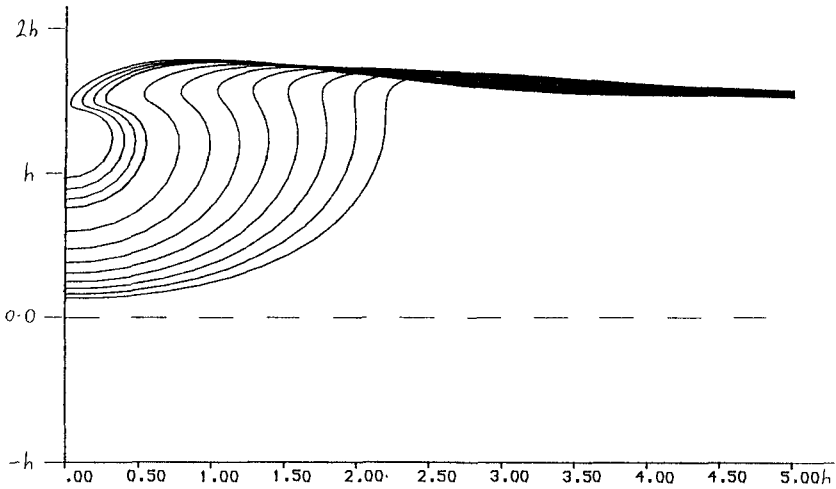


Figure 3: The wave of figure 2 meeting a wall as it overturns. The initial wall-wave distance,  $x_0 = 9$ . Surface profiles at  $t = 4$  (0.1) 4.8 (0.03) 4.89

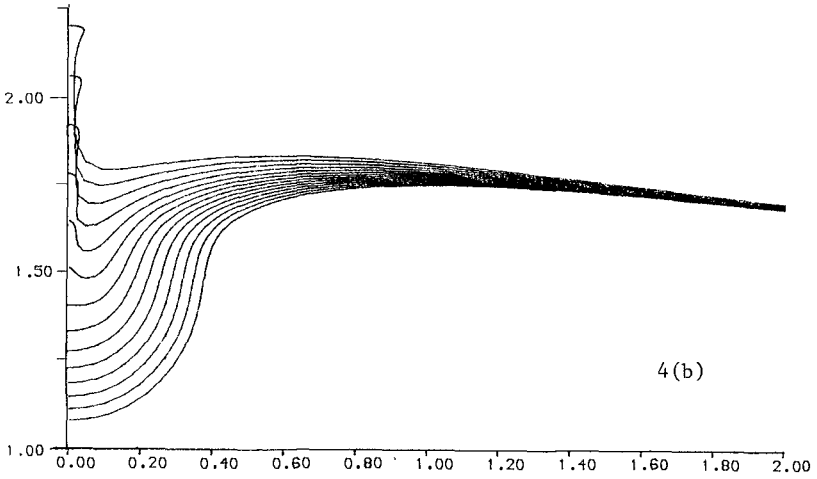
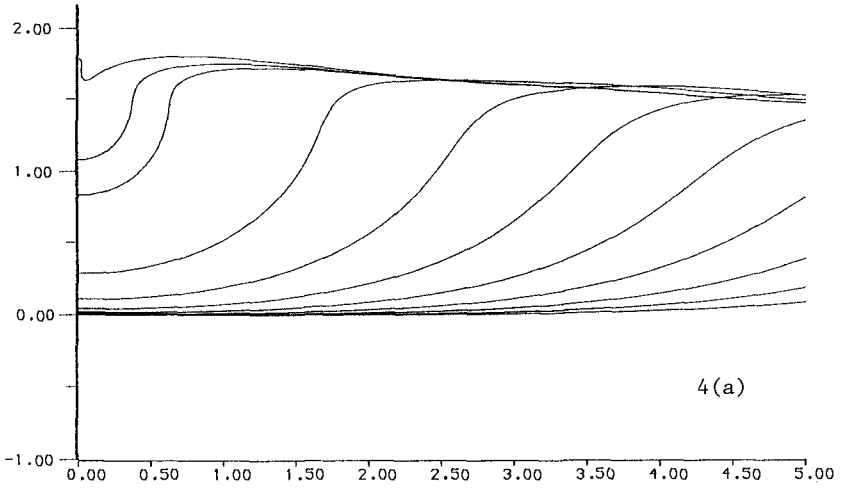


Figure 4:  
 The wave of figure 2 meeting a wall *before* it overturns ( $x_0=7.5$ ).  
 (a) Surface profiles at times  $t = 0$  (0.5) 4.0, 4.1, 4.2 .  
 (b) Close-up view near the water-line at times  $t = 4.10$  (0.01) 4.23

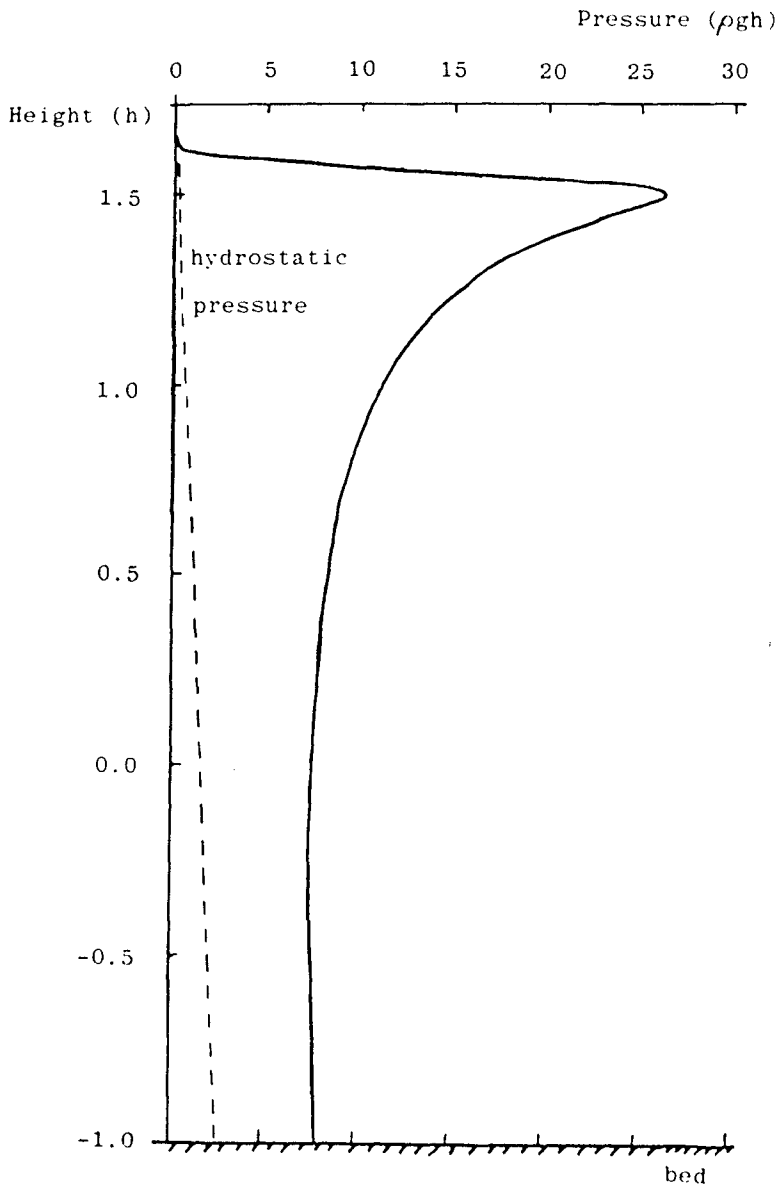


Figure 5: Pressure on the wall at time  $t = 4.19$ , for the wave in figure 4. This is the time of maximum pressure. The broken line shows the relatively small component of hydrostatic pressure.

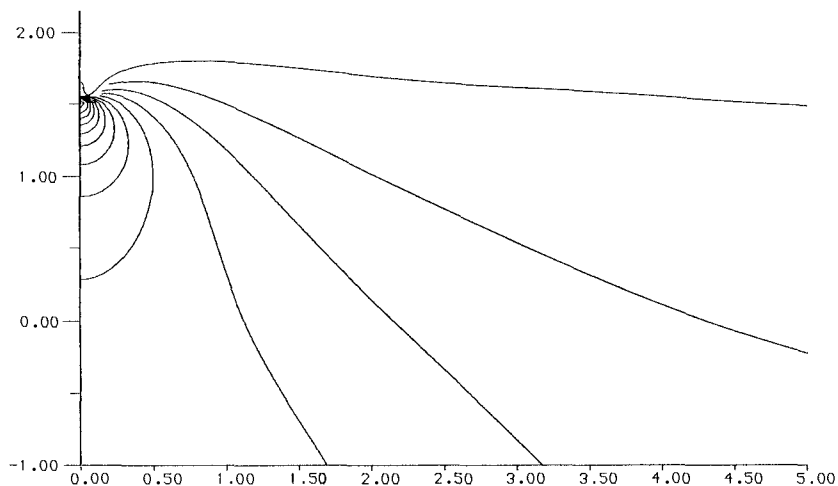


Figure 6: Pressure contours for the wave in figure 4 at time 4.19. The free surface has pressure zero. The pressure contour increment is  $2 \rho gh$ . The peak pressure is  $26 \rho gh$ , and lies just below the water-line.

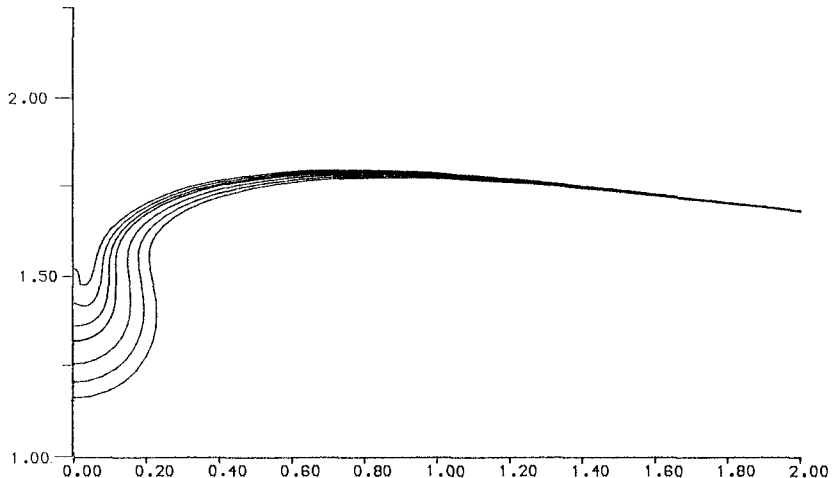


Figure 8: The wave of figure 2 meeting the wall, with  $x_0 = 8$ . Note that this is a close-up view near the water-line. Surface profiles at times  $t = 4.400 (0.01) 4.430 (0.005) 4.445$ .

Note this is drawn on the same spatial scale as figure 4(b).

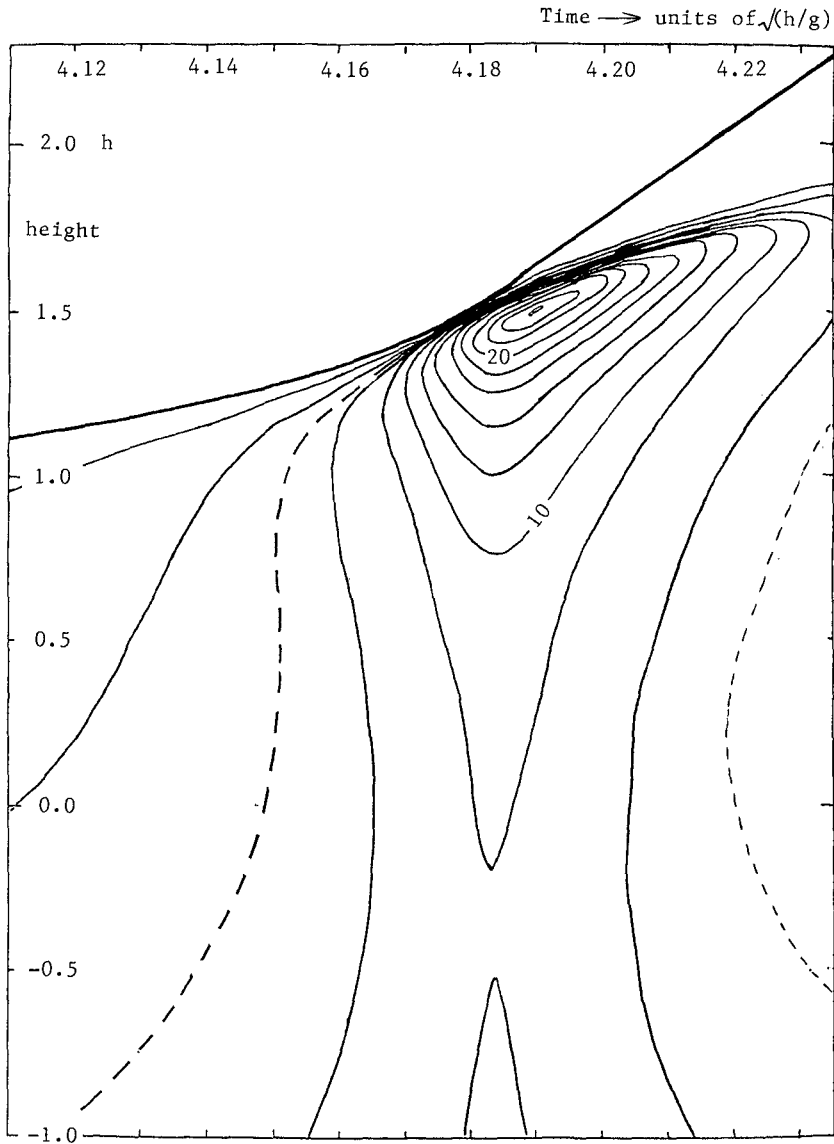


Figure 7: Pressure on the wall for the wave in figure 4. The pressure contours are drawn here as a function of *distance up the wall* (vertical axis) and *time* (horizontal axis). The solid upper curve is the position of the water-line. The contour interval is 2 pgh, except for the broken-line contour at 5 pgh.